analytical chemistry

Letter

pubs.acs.org/ac

Quantifying Ligand Adsorption to Nanoparticles Using Tandem Differential Mobility Mass Analysis

Suvajyoti Guha,[†,‡] Xiaofei Ma,[†,‡] Michael J. Tarlov,[‡] and Michael R. Zachariah*[,†,‡]

[†]University of Maryland, College Park, Maryland 20742, United States

[‡]National Institute of Standards and Technology, Gaithersburg, Maryland 20899, United States

Supporting Information

ABSTRACT: Although electrospray-differential mobility analyzers (ES-DMA) have been previously employed to characterize ligand binding to nanoparticles, absolute quantification of surface coverage can be inaccurate at times because of ligand conformational effects. In this Letter, we report a quantitative technique by in-flight coupling of a particle mass analyzer (APM) with ES-DMA, thus enabling a direct quantitative analysis of mass independent of particle size, material, morphology and conformation. We demonstrate the utility of ES-DMA−APM by studying two model complex systems (gold nanoparticle−bovine serum albumin and polystyrene bead−antibody) as a function of concentration and pH. Our results obtained with ES-DMA−APM are in excellent agreement with prior work. We anticipate that this will enhance the capabilities of online quantitative characterization of ligand binding to nanoparticles.

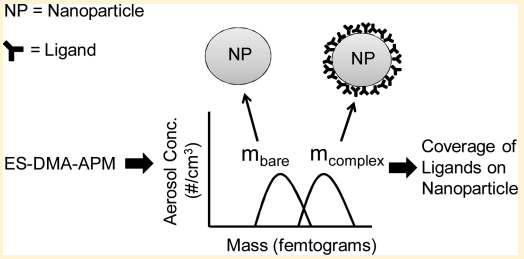

Quantifying protein adsorption to nanoparticles is important in the development of nanoparticle-based therapeutics and delivery systems.[1] Several methods are routinely used for quantifying protein adsorption to nanoparticles (or surfaces), including UV−vis,[2] fluorescence spectroscopy,[3] reflectometry,[4] quartz crystal microbalance (QCM-D),[5] surface plasmon resonance,[6] and ellipsometry.[7] More recently, electrospray-differential mobility analysis (ES-DMA)[8−11] has been exhibiting increased applications in this field. ES-DMA uses an electrospray system to first aerosolize nanoparticles and then characterize their electrical mobility by balancing electrical and drag forces on the particles.[12] By scanning through a range of electrical mobility distributions, each counted using a condensation particle counter, one obtains an equivalent spherical diameter distribution of the particle population. ES-DMA has been used to measure the size of a variety of nanoparticles, such as gold nanoparticles (Au NPs), viruses, and proteins; a comprehensive review of which can be found elsewhere.[13] ES-DMA has also been employed to characterize the number of proteins adsorbed to nanoparticles by measuring the decrease in electrical mobility of a complex particle (i.e., a particle with protein adsorbed on it) relative to the bare particle.[8−11] By assuming a size for the adsorbed protein, surface coverage can then be determined. Because this principle of ES-DMA is independent of material property, it could in general be used to characterize interactions between nanoparticles and proteins, viruses and proteins, protein and proteins, and viruses and quantum dots, etc. Thus, for generality in this paper, we define any particle adsorbing to a nanoparticle (or any analyte) as a ligand, and the resultant product is a complex.

Two different approaches using ES-DMA have been explored for quantifying ligands adsorbed to nanoparticles: an area-based (AB) approach and a volume-based (VB) approach[13] (Supporting Information S1). These two approaches typically do not yield the same result, with the AB approach yielding a significantly smaller ligand density than the VB method (Supporting Information S2).[13] This inconsistency presumably results because to extract ligand coverage, some a priori knowledge of ligand conformation is required. It is commonly assumed that a ligand retains its solution conformation upon binding; however, several studies suggest that proteins may undergo conformational changes upon adsorption.[14−16]

An alternative to these approaches is a direct mass measurement of ligand adsorption, thereby eliminating the need to assume a shape for ligands. The relatively high mass of nanoparticle complexes can be determined using an aerosol particle mass analyzer (APM).[17] The APM is a fundamental mass measurement device that determines mass by a balance of electrical and centrifugal forces.[17] A powerful approach for nanoparticle characterization is to serially combine APM with DMA. This tandem DMA−APM approach enables size selection with a DMA and a subsequent mass measurement of the size-selected particle. In this combination, the DMA−APM has been used to measure the density of carbon nanotubes,[18] the porosity of nanoparticles,[19] the effective density of soot,[20] and the mass and density changes of metal nanoparticles undergoing oxidation.[21]

Received: May 23, 2012
Accepted: July 5, 2012
Published: July 5, 2012

dx.doi.org/10.1021/ac301149k | *Anal. Chem.* 2012, 84, 6308−6311

In this letter, we demonstrate that the combination of ES-DMA and APM can be used to quantify ligand adsorption to nanoparticles. We provide two model examples: bovine serum albumin (BSA) adsorption to 30 nm gold nanoparticles (Au NPs) and Rituximab (RmAb, a therapeutic monoclonal antibody) adsorption to 60 nm polystyrene latex (PSLs) nanoparticles. Details about the sample preparations are available in the Supporting Information (S3). Although we focus only on protein adsorption to nanoparticles, the principles demonstrated here are independent of nanoparticle and ligand properties and, hence, can be used for any type of bionanoparticle complexes. With our current configuration, the ES-DMA–APM can detect protein coatings as low as 5% of a monolayer of IgG on PSLs and 20% of a monolayer of BSA on Au NPs (Supporting Information S3). It should be pointed out that nonvolatile buffers or other modifiers may pose a problem during analysis with ES-DMA–APM because they may remain in the same ES droplet and can affect the measured final size and mass of the analyte. To overcome this problem, the complexes can be centrifuged, diluted, or exchanged with volatile buffers through dialysis.

The approach used for quantifying ligand coverage using ES-DMA–APM is depicted in Figure 1. Further details about

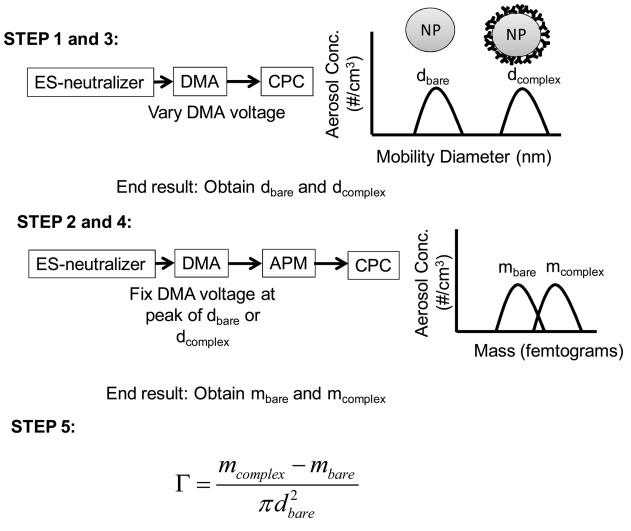

Figure 1. Steps using ES-DMA–APM system to determine the ligand coverage per nanoparticle.

instrument operating conditions are provided in the Supporting Information (S3). The first step is a direct measurement of the bare sample size distribution (say, Au NPs or PSLs) by scanning the DMA voltage to obtain the mobility size (step 1, Figure 1). The DMA voltage is then set at the peak of the size distribution of the particles to extract only particles with a selected mobility, which are then sent to the APM, where the mass distribution is measured (step 2, Figure 1). This step is then repeated for the complex to obtain the mass of the peak size of the complex (steps 3 and 4, Figure 1). The coverage of the ligands is then obtained by dividing the mass of the adsorbed ligands by the mobility area of the bare nanoparticle (step 5, Figure 1).

Using this approach, the amount of protein adsorbed was calculated for AuNP-BSA samples as a function of increasing BSA concentration. The results obtained with ES-DMA–APM are shown in Figure 2, where the coverage of BSA is observed to increase with concentration, a behavior that has been

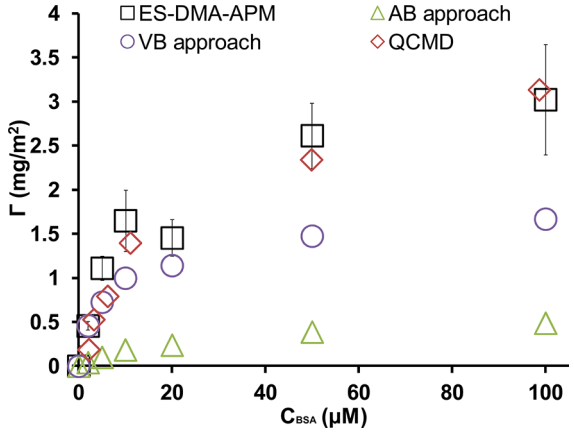

Figure 2. Coverages of BSA on 30 nm AuNP as a function of concentration obtained with ES-DMA–APM (square-black) predictions based on AB (triangle-green) and VB approach (circle-purple) and comparisons with data obtained on planar Au surface using QCM-D (diamond-red). The error bars are from measurements made at least in duplicate.

previously reported for several other proteins on different surfaces.[22−25] Using results solely from ES-DMA measurements, the coverage of BSA on AuNPs can be determined using the AB and VB approaches (Supporting Information S1). Comparing the two approaches (Figure 2), it is evident that the AB approach consistently underreports compared with the VB approach. In contrast, the VB approach shows reasonable agreement at low concentrations but starts to underreport the amount of ligand adsorbed significantly at higher concentrations of BSA. One possible explanation for the good agreement at low concentrations for the VB approach is that at lower concentrations of added BSA, the protein assumes a more expanded (Supporting Information S1) conformation. As already mentioned, this is not surprising because others have also reported that different proteins can assume expanded conformations at lower concentrations.[14,15,26] As the concentration increases, more BSA molecules apparently assume a more compact conformation, and the VB approach deviates from the ES-DMA–APM results.

Our values obtained with DMA–APM are in excellent agreement with coverages of BSA obtained on a planar Au surface using QCM-D in 10 mM sodium citrate buffer at pH 8.55,[5] as shown in Figure 2, and also provide a good Langmuir isotherm fit (Supporting Information S4, Figure S1). The agreement with QCM-D implies that BSA adsorption to 30 nm nanoparticles is similar to that on planar surfaces, which is not unreasonable because several studies appear to suggest that ligand adsorption is independent of particle size, especially for particle sizes >30 nm.[8,27] The similarity in the results between ES-DMA–APM and QCM-D also implies that the adsorption of BSA is not strongly influenced by the differences in the buffer used, their ionic strengths, and the differences in pH.

In a second application, we determined the adsorption of RmAb on polystyrene latex (PSLs) nanoparticles. In these experiments, the coverage of RmAb adsorbed on 60 nm PSL nanoparticles as a function of pH was determined using ES-DMA–APM (Supporting Information S4, Figure S2). The coverage reaches a maximum at pH ≈ 8.5 which is close to the isoelectric point (pI) of RmAb.[28] There are at least two possibilities that may explain the maximum coverage near the pI: (i) net zero charge of a RmAb molecule would mean the

dx.doi.org/10.1021/ac301149k | Anal. Chem. 2012, 84, 6308−6311

decreased electrostatic repulsions between neighboring molecules allows for more compact packing on the surface and (ii) the RmAb molecules interact with each other and the PSL surface through hydrophobic interactions; denature significantly; and promote nonspecific adsorption of more RmAb molecules, creating multiple layers. The coverage decreases rapidly in moving to higher or lower pH values relative to the pI. Quantifying the amount adsorbed with ES-DMA–APM enables comparisons with values predicted by VB and AB approaches. Consistent with the observations discussed for BSA adsorbed to Au NPs, it is found the AB approach underreports significantly at all pH values, whereas VB appears to corroborate well with ES-DMA–APM at low pH values (~5) but negatively deviates at higher pH, especially when adsorption is multilayered (arguments for the number of protein layers are available in Supporting Information S4).

To compare the pH-dependent adsorption behavior of RmAb with that of different antibody–particle systems reported by others, we plot adsorption coverage versus a pH scale relative to the pI of each antibody, as shown in Figure 3.

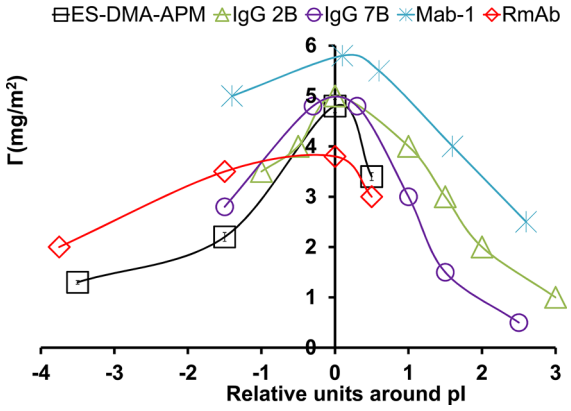

Figure 3. RmAb adsorbed on 60 nm PSL (NIST SRM 1964) as a function of pH (scale relative to pI) quantified with ES-DMA–APM (square, black) and comparisons with published results for IgG 2B (mouse IgG type 1, pI 5.0)[29] (triangle, green); IgG 7B (mouse IgG type 1, pI 5.5)[29] (circle, purple); Mab-1 (pI 5.4)[30] (asterisk, blue) on negatively charged 297 nm polystyrene beads using acetate buffer at pH 4 and 5, phosphate buffer at pH 6 and 7, and borate buffer at pH 8, 9, and 10, respectively; and RmAb (pI 8.5)[28] (red, diamond) on negatively charged silica surface (diamond, red) using ammonium acetate buffer. Lines are for guiding the eyes only. The error bars are from measurements made at least in duplicate.

On the basis of the results obtained with other type-1 immunoglobulins (IgG 2B,[29] IgG 7B,[29] Mab-1,[30] and RmAb[28]) on nanoparticles and planar surfaces, it is evident that the dome-shaped adsorption pattern for RmAb is similar to that observed for monoclonal IgGs with different techniques implying that electrostatic forces (between protein–protein and protein-sorbent) play an important role in determining coverage.

In summary, by integrating an APM with the conventional ES-DMA, we show that ES-DMA–APM can be used for quantifying ligand adsorption to nanoparticles. This approach was demonstrated using two model nanoparticle–protein complex systems: AuNP-BSA and PSL-RmAb. The use of the APM also allowed for a more systematic investigation of potential biases of the AB and VB approaches that can be used for quantification by ES-DMA. Our results indicate that both AB and VB methods report lower coverage values relative to those determined by APM, with AB values being the lowest. The foremost advantage of ES-DMA–APM is (a) that it can also be used for heterogeneous samples (constituting bare particles of different sizes) as long as the resolution of the APM is sufficiently high and (b) it is independent of the nanoparticle and ligand type, shape, and size. The generic nature of the method suggests it can be applied for a wide range of complexes (such as adsorption of peptides, proteins, quantum dots, etc. to different types of nanoparticles such as viruses, gold, silver, etc).

■ ASSOCIATED CONTENT

Supporting Information

Governing equations for quantifying ligand adsorption to nanoparticles, comparison of AB approach and VB approach from literature, materials and methods, estimation of number of layers of proteins adsorbed, figure of Langmuir isotherm fit of coverage of BSA adsorbed to 30 nm AuNPs as a function of concentration and figure of coverages obtained with ES-DMA–APM and predicted by AB and VB approaches for RmAb-PSL complexes as a function of pH. This material is available free of charge via the Internet at http://pubs.acs.org.

■ AUTHOR INFORMATION

Corresponding Author

*E-mail: mrz@umd.edu.

Notes

The authors declare no competing financial interest.

■ REFERENCES

(1) Thobhani, S.; Attree, S.; Boyd, R.; Kumarswami, N.; Noble, J.; Szymanski, M.; Porter, R. *J. Immunol. Methods* **2010**, *356* (1–2), 60–69.
(2) Larsericsdotter, H.; Oscarsson, S.; Buijs, J. *J. Colloid Interface Sci.* **2001**, *237* (1), 98–103.
(3) Weiss, S. *Science* **1999**, *283* (5408), 1676–1683.
(4) Buijs, J.; vandenBerg, P. A. W.; Lichtenbelt, J. W. T.; Norde, W.; Lyklema, J. *J. Colloid Interface Sci.* **1996**, *178* (2), 594–605.
(5) Brewer, S. H.; Glomm, W. R.; Johnson, M. C.; Knag, M. K.; Franzen, S. *Langmuir* **2005**, *21* (20), 9303–9307.
(6) Mrksich, M.; Sigal, G. B.; Whitesides, G. M. *Langmuir* **1995**, *11* (11), 4383–4385.
(7) Tengvall, P.; Askendal, A.; Lundstrom, I. *Colloids Surf., B* **2001**, *20* (1), 51–62.
(8) Tsai, D. H.; Delrio, F. W.; Keene, A. M.; Tyner, K. M.; Maccuspie, R. I.; Cho, T. J.; Zachariah, M. R.; Hackley, V. A. *Langmuir* **2011**, *27* (6), 2464–2477.
(9) Yim, P. B.; Clarke, M. L.; McKinstry, M.; De Paoli Lacerda, S. H.; Pease, L. F., III; Dobrovolskaia, M. A.; Kang, H.; Read, T. D.; Sozhamannan, S.; Hwang, J. *Biotechnol. Bioeng.* **2009**, *104* (6), 1059–1067.
(10) Laschober, C.; Wruss, J.; Blaas, D.; Szymanski, W. W.; Allmaier, G. *Anal. Chem.* **2008**, *80* (6), 2261–2264.
(11) Pease, L. F.; Tsai, D. H.; Zachariah, M. R.; Tarlov, M. J. *J. Phys. Chem. C* **2007**, *111* (46), 17155–17157.
(12) Knutson, E. O.; Whitby, K. T. *J. Aerosol Sci.* **1975**, *6*, 443–451.
(13) Guha, S.; Li, M.; Tarlov, M. J.; Zachariah, M. R. *Trends Biotechnol.* **2012**, *30* (5), 291–300.
(14) Norde, W.; Favier, J. P. *Colloids Surf.* **1992**, *64* (1), 87–93.
(15) van der Veen, M.; Stuart, M.; Norde, W. *Colloids Surf., B* **2007**, *54* (2), 136–142.
(16) Hook, F.; Rodahl, M.; Kasemo, B.; Brzezinski, P. *Proc. Natl. Acad. Sci. U.S.A.* **1998**, *95* (21), 12271–12276.

(17) Ehara, K.; Hagwood, C.; Coakley, K. *J. Aerosol Sci.* **1996**, *27* (2), 217−234.
(18) Kim, S. H.; Mulholland, G. W.; Zachariah, M. R. *Carbon* **2009**, *47*, 1297−1302.
(19) Lee, S.; Chang, H.; Ogi, T.; Iskandar, F.; Okuyama, K. *Carbon* **2011**, *49* (7), 2163−2172.
(20) Park, K.; Kittelson, D.; Zachariah, M.; McMurry, P. *J. Nanopart. Res.* **2004**, *6* (2−3), 267−272.
(21) Ma, X.; Lall, A.; Mulholland, G.; Zachariah, M. *J. Phys. Chem. C* **2011**, *115* (34), 16941−16946.
(22) Jonsson, U.; Malmqvist, M.; Ronnberg, I. *Biochem. J.* **1985**, *227* (2), 373−378.
(23) Silva, C. S. O.; Baptista, R. P.; Santos, A. M.; Martinho, J. M. G.; Cabral, J. M. S.; Taipa, M. A. *Biotechnol. Lett.* **2006**, *28* (24), 2019−2025.
(24) Chuang, H. Y. K.; King, W. F.; Mason, R. G. *J. Lab. Clin. Med.* **1978**, *92* (3), 483−496.
(25) Fair, B. D.; Jamieson, A. M. *J. Colloid Interface Sci.* **1980**, *77* (2), 525−534.
(26) Ball, V.; Bentaleb, A.; Hemmerle, J.; Voegel, J. C.; Schaaf, P. *Langmuir* **1996**, *12* (6), 1614−1621.
(27) Teichroeb, J.; Forrest, J.; Jones, L. *Eur. Phys. J. E* **2008**, *26* (4), 411−415.
(28) Guha, S.; Wayment, J. R.; Li, M. D.; Tarlov, M. J.; Zachariah, M. R. *Langmuir* **2011**, *27* (21), 13008−13014.
(29) Elgersma, A. V.; Zsom, R. L. J.; Norde, W.; Lyklema, J. *Colloids Surf.* **1991**, *54* (1−2), 89−101.
(30) Galisteo-Gonzales, F.; Martin-Rodriguez, F.; Hidalgo-Alvarez, R. *Colloid Polym. Sci.* **1994**, *272* (3), 352−358.